

Original Research

Influence of Loess Interlayer Thickness on Water Transport in Sand

Chao Wu^{1,2}, Yinli Bi^{1,2,3*}, Peter Christie¹

¹Institute of Ecological Environment Restoration in Mine Areas of West China, Xi'an University of Science and Technology, Xi'an 710054, China

²College of Geology and Environment, Xi'an University of Science and Technology, Xi'an 710054, China

³Institute of Mine Ecological Restoration, China University of Mining and Technology (Beijing), Beijing 100083, China

Received: 29 October 2021

Accepted: 27 January 2022

Abstract

The texture of the soil profile determines the movement and distribution of soil water and also affects plant growth and development. Most studies have focused on the movement of water in homogeneous or layered soil profiles such as coarse sand or gravel as a capillary barrier. Few studies have used loess as an interlayer of sand to study the water distribution characteristics of soil profiles. Here, a layered sand-loess-sand soil profile was constructed in indoor soil columns to explore the effects of different thicknesses of loess interlayer (0, 10 and 20 cm) on water transport. The advancing height of the sand wetting front followed a power function with time in different loess interlayer thickness treatments and the loess interlayer promoted the advancing height of the wetting front. Loess interlayer treatment significantly increased the soil volumetric water content in the corresponding treatment layer (40-60 cm). The thicker the loess interlayer the higher the soil volumetric water content. After two months of soil drainage the volumetric water content in the treatment layer (40-60 cm) corresponding to the loess interlayer treatment did not decline but the control declined by 1.36%. These results may provide a scientific basis and theoretical support for the artificial reconstruction of soil profiles in arid and semi-arid coal mining areas to optimize sand moisture content.

Keywords: water distribution, loess interlayer, soil volume water content, sand

Introduction

Coal accounts for about 70% of primary energy production and consumption in China and has long been a dominant energy source [1, 2]. Increasing coal mining activity has degraded the surface ecology and environment and damaged the groundwater system,

thereby aggravating the fragility of the surface ecology and the shortage of groundwater resources [3-5]. The efficiency of ecological reconstruction has been greatly restricted by a lack of water resources. Investigation of methods to maximize the use of shallow groundwater by plants has therefore become an urgent task [6-8].

Soil texture strongly determines the water-holding capacity of soils and also affects other hydraulic properties such as permeability and hydraulic conductivity [9]. Soil hydraulic properties play an important role in regulating the balance of water and

*e-mail: ylbi88@126.com

nutrients in agricultural ecosystems [10]. In addition, soil moisture has a major impact on fundamental ecological properties such as biomass [11, 12] and carbon sequestration [13]. Optimizing soil texture affects the distribution of soil water and nutrients and thus affects the growth and development of plants. Soil reconstruction is usually conducted with homogeneous or layered soil and the texture of the reconstructed soil directly determines its hydraulic properties. Even with stable groundwater table depth and other environmental conditions the hydraulic relationship between shallow soil and groundwater may change substantially due to differences in soil hydraulic properties [14]. Most early studies were based on the assumption that the soil was homogeneous because of the complexity of water dynamics in heterogeneous porous media, but a truly homogeneous soil is difficult to find in practical studies [15]. Sand is usually employed in arid and semi-arid areas and a reconstructed soil profile consisting of homogeneous sand is not conducive to ecological restoration. Layered soils with different particle sizes are therefore widely used in soil profile reconstruction in open-pit mining areas [16-18]. A good understanding of the soil texture and stratification characteristics of the soil profile is very important in terms of soil water evaporation and water distribution.

At present the establishment of a soil interlayer is a common method of achieving a good water distribution in the soil profile [19]. Most studies have examined the movement characteristics of water in homogeneous or some special layered soil profiles. For example, Yan et al. [20] established a gravel layer under a loess layer and found that the interlayer significantly affected the infiltration of surface water. In other studies, a coarse sand layer has been used as an interlayer to study its influence on water and salt transport [21, 22]. However, numerous theoretical and experimental studies have been conducted on layered soil profiles but few have used loess as an interlayer of sand to study the water distribution characteristics of the soil profile formed and whether this has effectively increased the soil water content. A reconstructed layered soil profile comprising sand-loess-sand is different from other layered soil profiles and it is therefore necessary to carefully study the influence of its characteristics on water distribution. This is especially important in the artificial construction of a layered soil profile to enhance the ecological status of sand in the land reclamation of arid and semi-arid mining areas. In addition, due to the large scale and high cost of soil profile reconstruction, indoor soil

column tests can be used to minimize uncontrollability, save costs, and provide reliable results and a theoretical basis for engineering practice [23].

Here, loess has been studied as an interlayer of sand using indoor soil column tests. The main purposes were (1) to reveal the effect of loess interlayer thickness on sand water transport, (2) to determine whether the reconstructed soil profile can increase soil water content, and (3) to examine the water retention characteristics of loess interlayers of different thickness under drainage conditions.

Materials and Methods

Test Materials

The sand used in the test was taken from fresh river sand and treated by air-drying and sieving (2 mm). The sand with grain size greater than 0.5 mm accounts for 56.83% of the total content, which belonged to coarse sand. The test loess was collected from Jingyang county, Shaanxi province, northwest China. The loess was crushed in a sample grinder, dried, sieved (2 mm) and thoroughly mixed. The physical and chemical properties of the soil are shown in Table 1. The grain size distribution of sand and loess is shown in Fig. 1.

Test Device and Steps

The test device was a column composed mainly of plexiglass with a moisture monitoring system and water supply facilities as shown in Fig. 2. The column was 125 cm high and 20 cm in diameter. The bottom was closed and the top was open. Monitoring holes with a diameter of 1 cm were drilled in a vertical line 0, 30, 40, 50, 60, 70, 80, 90 and 100 cm from the bottom of the column. The top of the underground aquifer was recorded as the 0 point of the height of the soil column for convenience in subsequent analysis and to 80 cm on the surface of the soil column, water sensors were embedded through the monitoring holes every 10 cm and connected to an external data collector. Table 2 shows details of the moisture monitoring system. A stable and continuous water supply to the soil column was maintained using a Mariotte bottle (height 30 cm, diameter 10 cm) to maintain the stability of the aquifer at the bottom of the soil column.

A layer of quartz sand 20 cm thick (quartz sand with diameters of 1-2, 2-4, 4-8 and 8-16 cm from top

Table 1. Physicochemical properties of soil and loess.

Soil texture	Grain size content/%			pH	Electrical conductivity ($\mu\text{s}\cdot\text{cm}^{-1}$)
	2-0.1 mm	0.1-0.01 mm	< 0.01 mm		
Sand	85.4	12.8	1.8	8.9	50.51
Loess	14.6	77.2	8.2	8.6	110.2

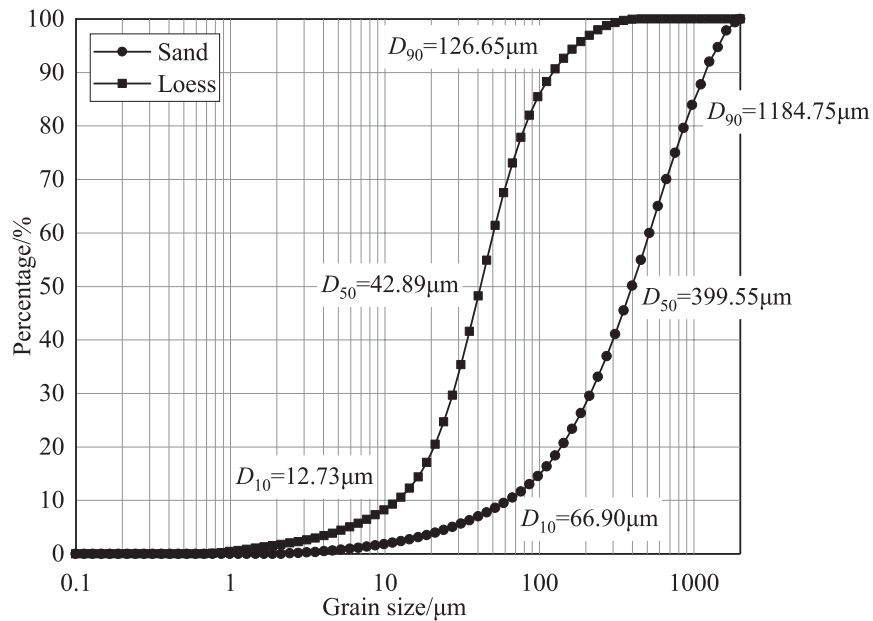


Fig. 1. Grain size distribution curves of sand and loess.

to bottom) was placed in the bottom of the column before the soil was transferred to simulate the aquifer. A geotextile with the same cross-sectional area as the soil column was placed on the top of the quartz sand layer to prevent the upper soil grains from entering the aquifer. The test soil was introduced onto the quartz sand layer according to the design bulk density

(sand, 1.6 g·cm⁻³, loess 1.3 g·cm⁻³) and compacted in layers of 5 cm to avoid layering of the soil. A layer of 25 cm remained empty at the top of the soil column for follow-up test simulation. The position of the Mariotte bottle remained unchanged throughout this process and changes in water level during the test were recorded.

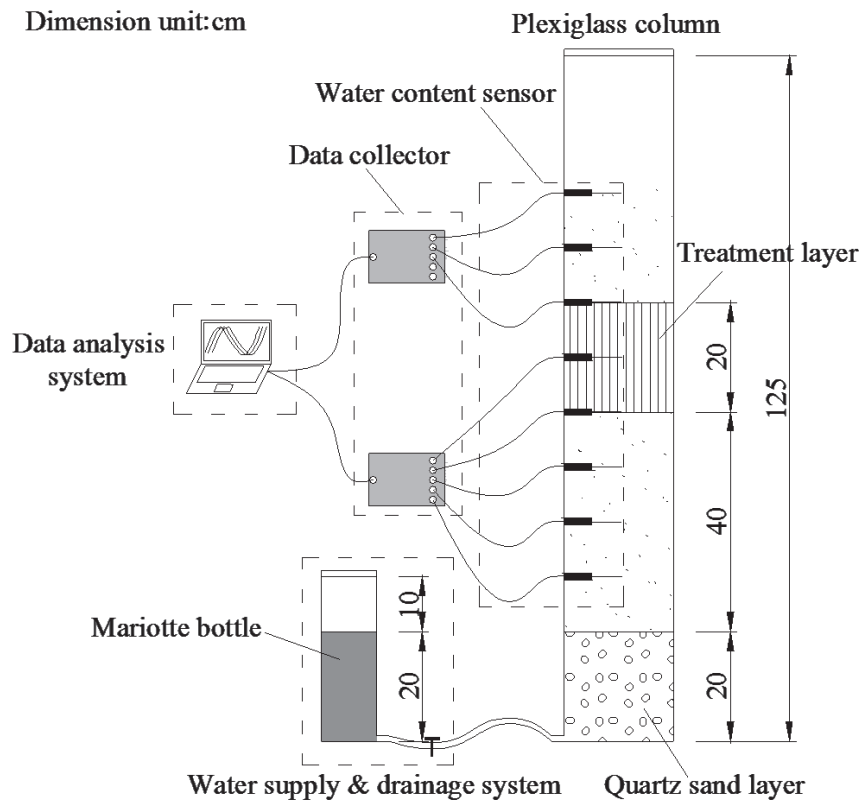


Fig. 2. Schematic diagram of test device.

Table 2. Details of the moisture monitoring system.

Test instrument	Features
Data collector	Decagon EM50 data logger (Meter Group, Brisbane, Australia) with five channels and a minimum measurement frequency that can meet the reading requirement of data per minute.
Water content sensor	Decagon 5TE soil moisture sensor with simultaneous measurement of volumetric moisture content, temperature and conductivity with errors of $\pm 1\text{-}2\%$, $\pm 1^\circ\text{C}$ and $\pm 10\%$, respectively.



Fig. 3. Test treatment design of soil columns. A: CK, no loess layer; B: LS, containing loess at 40-50 cm and sand at 50-60 cm; C: LL, containing loess at 40-60 cm.

Test design

Three treatments were set up in the soil 40-60 cm above the top of the column aquifer as follows; first, a control with a 20-cm sand layer but no loess layer (designated CK); second, a 10-cm loess layer and a 10-cm sand layer (LS); and third, a 20-cm loess layer (LL). The test treatment design is shown in Fig. 3.

Test Operation

Capillary water rise test. Water was added to replenish the Mariotte bottles to the top water level of the quartz sand layers. The capillary water rose rapidly at first and when the wetting front reached below the treatment layer the position of the wetting front was recorded every five minutes and the measurement frequency of the sensor was set to collect data every minute. When the wetting front reached the treatment layer and above the position of the wetting front was recorded every two hours and the frequency of measurement by the sensor was set to every hour. The drop in water level in the Mariotte bottle and the quantity of water consumed were recorded simultaneously. The test was conducted at a controlled temperature of 20-24°C and evaporation from the soil column and Mariotte bottle was prevented. The test started on 14/11/2020 and ended on 14/1/2021.

Soil water retention test. After the capillary water rose and stabilized the Mariotte bottle was removed and the water supply stopped so that the soil water could drain naturally from the bottom outlet hole. The top cover of the soil column was opened to simulate the soil drainage process under natural evaporation conditions.

The measurement frequency of the sensor was set to collect data every hour. The test started on 14/1/2021 and ended on 14/3/2021.

Results and Analysis

Advancing Height of Wetting Front

Fig. 4 shows the change in wetting front with time in the different treatments. The relationship between

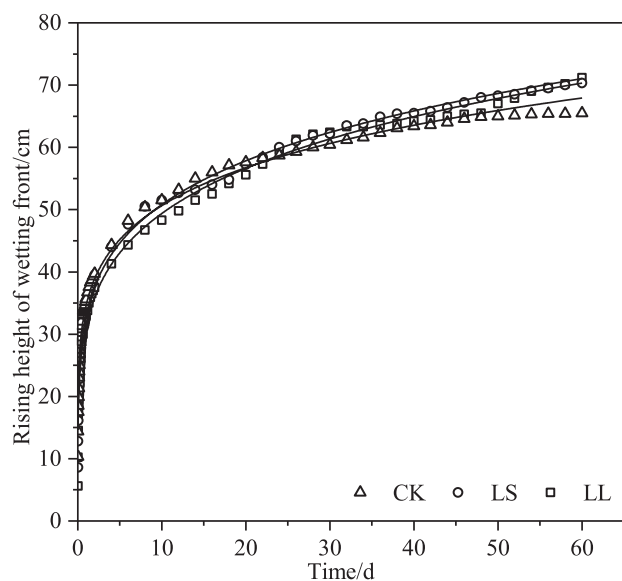


Fig. 4. Variation in wetting front with time under the different treatments.

Table 3. Fitting equation between advancing height of wetting front and time under the different treatments.

Treatment	Fitting relationship ¹⁾	R ²
CK	$H = 34.7217t^{0.1639}$	0.9844
LS	$H = 33.0228t^{0.1871}$	0.9904
LL	$H = 31.3455t^{0.1974}$	0.9881

¹⁾H, advancing height of wetting front, cm; t, time required, d.

the advancing height of the wetting front and time was a power function ($H = at^b$) and the fitting equation is shown in Table 3. Below 40 cm the wetting front in the loess layer treatment was the same as in the control and the advancing height curve of the wetting front coincided well within 3 d. In the control and the LS treatment the time taken for the wet front to reach the bottom surface (40 cm) of the treatment layer was ~2d and that in the LL treatment was 3.25 d as shown in Table 2.

In the different loess layer thickness treatment the time taken by the wetting front to go through the treatment layer (40-60 cm) was significantly lower than CK (Table 2) and the time followed the sequence: CK>LS>LL. The times in treatments LS and LL were significantly (4.09 and 4.88d) lower than CK. The migration rate of the wet front through the treatment layer (40-60 cm) followed the sequence LL>LS>CK. In treatments LL and LS the times required for the wetting front to reach 70 cm were 56.5 and 57d with no significant difference, but CK reached only 66.3 cm in contrast to treatments LS and LL. Thus, the advancing height of the different thickness loess layer treatments (LS and LL) was greater than that of CK, and the times required to reach 70 cm were also significantly shorter than that of CK.

Migration Rate of Wetting Front

Fig. 5 shows the relationship between capillary water migration rate and time in different stages. Changes in capillary water migration rate in the three treatments with time were similar, with a more rapid migration rate at the initial stages of the test and a gradual decrease to zero with increasing time. The initial migration rate of capillary water in the soil columns was faster, especially on the first day, and the average migration rate across the three treatments was 34.6 cm·d⁻¹. The migration rate decreased rapidly with increasing time. At 1-4 d the migration rate of capillary water was 2.77-2.90 cm·d⁻¹, accounting for only 8.00-8.37% on the first day, and the rate decreased rapidly. After 10 d of the test the migration rate of capillary water was <1.0 cm·d⁻¹. In addition, comparing the three treatments, at the start of the test the migration rate in CK was slightly faster than in the two experimental treatments, but after 4 d the migration rates of LL and LS were higher than that CK. After 50 d the migration rate in LL was significantly higher than that in LS.

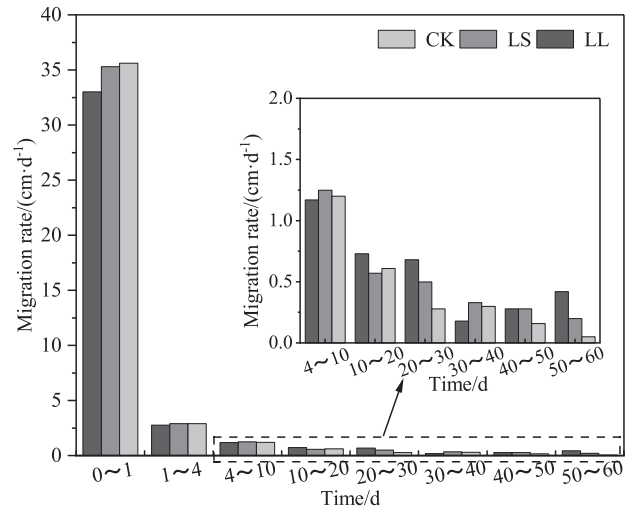


Fig. 5. Relationship between capillary water migration rate and time.

The migration rates of different loess thickness treatments (LS and LL) were slightly lower than that of CK initially stage, but the migration rates at later stages were higher than CK, especially that in LL.

Soil Profile Water Distribution

Fig. 6 shows the changes in volumetric water content of column soil profiles in the different treatments. The volumetric water content decreased gradually with increasing column height but the volumetric water contents of LS and LL in the treatment layer (40-60 cm) increased significantly, 11.2 and 18.5% higher than CK, and the volume water content followed the sequence LL>LS>CK. In the sand layer <40 cm there was no significant difference between treatments. The water content in the topsoil layer (60-80 cm) was low and close to the initial water content. LS and LL treatments could significantly increased the soil volumetric water content in the treatment layer (40-60 cm).

The water retention effect of the loess layers was studied by aquifer drainage after the depletion of the underground aquifers and the soil profile water contents in different treatments after one and two months of drainage were obtained. As shown in Fig. 7, the volumetric water content of soil columns at different heights increased from the start to the end of the water supply. Then after two months of drainage the volumetric water content of the soil at different heights gradually decreased. Comparing the soil water contents when the water supply stopped and after two months the drainage, the average water content of LS and LL in the treatment layer (40-60 cm) decreased by 0.21% and 0.31%, respectively, and CK decreased by 1.36%.

In conclusion, the soil volumetric water contents of LS and LL in the treatment layer (40-60 cm) increased significantly. After drainage for two months

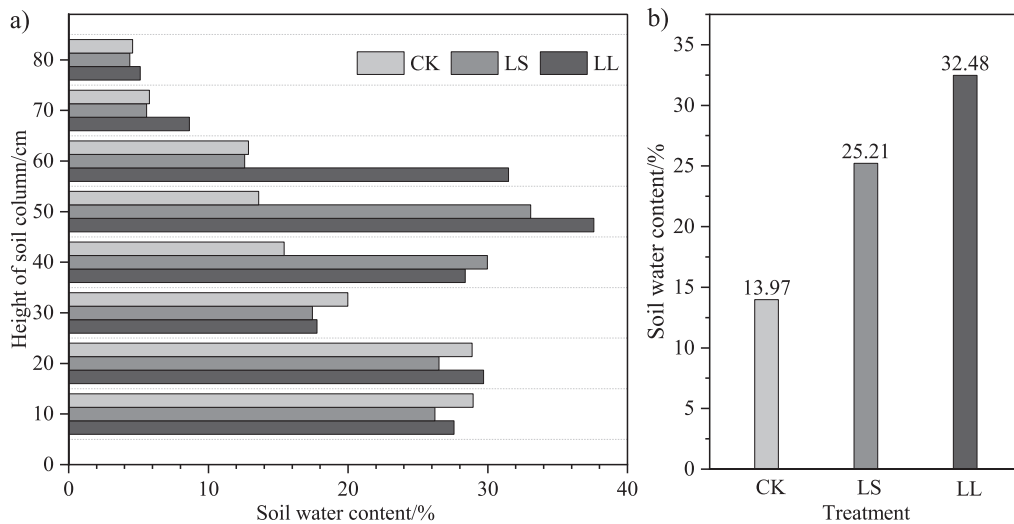


Fig. 6. Volumetric water content of soil profiles under the different treatments. A, the distribution of soil volume water content; B, the volumetric water content of different treatments in the treatment layer (40-60 cm). i.e., the mean value of volumetric water content at 40, 50 and 60 cm of the soil column.

the volumetric water content in the loess layer treatments (LS and LL) did not decrease, indicating that the loess interlayers provided water storage and produced a water retention effect.

Discussion

There is little rainfall and substantial evaporation in arid and semi-arid mining areas in western China [24, 25]. The groundwater system has been damaged by continuing increases in coal mining activity.

Plants are often subjected to drought stress, resulting in yield reductions and death over a large area [26]. In arid environments the groundwater is an important source of water for plant growth and survival [7, 27, 28]. Groundwater can rise to the root zone of plants through capillary forces to enable plant survival [29]. Here, loess has been used as an interlayer of sand to determine whether it can increase the water content in the soil profile.

A loess layer did increase the advancing height of the wetting front and the time required to rise to a certain height was also reduced (Fig. 4 and Table 2).

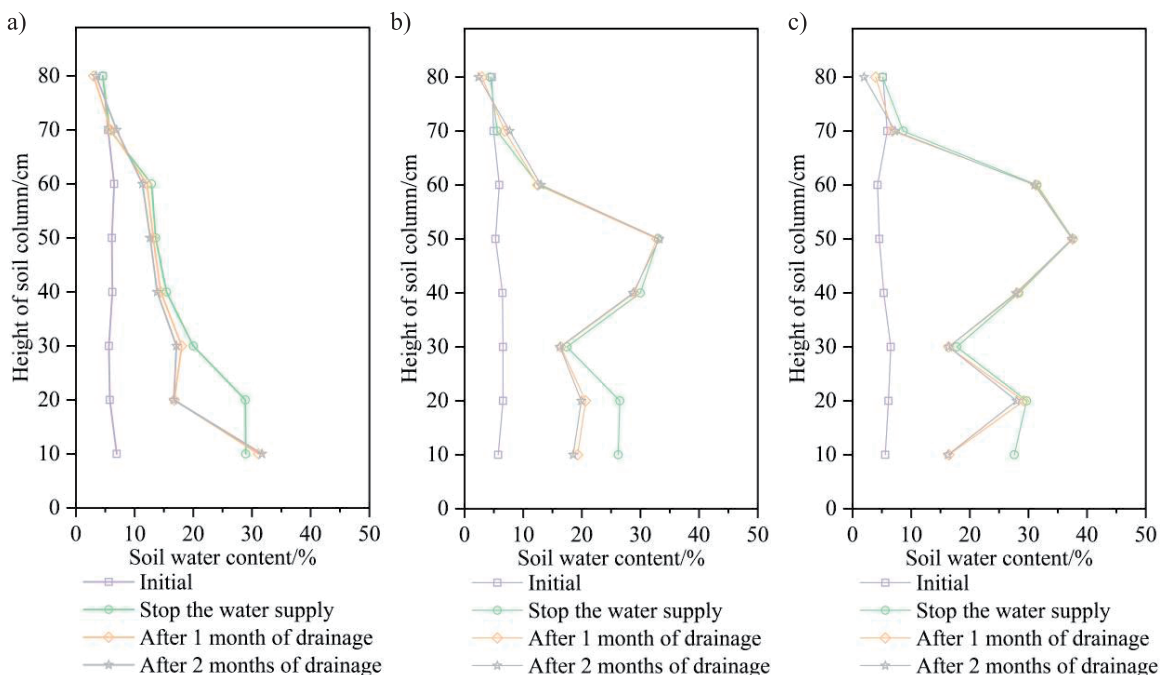


Fig. 7. Volumetric water content of the soil profile at different times. A, CK treatment; B, LS treatment; and C, LL treatment.

Table 4. Time taken to advance height of wetting front under the different treatments.

Treatment	Time to advance height to 40 cm (d)	Time to advance height to 60 cm (d)	Time to advance height to 70 cm (d)
CK	2.04	28.00	/ ¹⁾
LS	2.13	24.00	57.00
LL	3.25	24.33	56.50

¹⁾, has not risen to 70 cm.

This is similar to the previous research results, but the way of adding fine-grained materials is different. Found that with the increase of fly ash content, the maximum rising height of wetting front also increased linearly [30]. The migration of the wetting front is related to the soil matrix potential, gravity potential and temperature potential [31, 32]. In unsaturated soils under natural conditions, soil water transport is mainly affected by the matrix and gravity potentials [31]. Under the same experimental conditions the gravity and temperature potentials of each treatment were similar, and the advancing height of the wetting front depended largely on the size of soil matrix potential. Loess has a high silt content and its matrix potential is greater than that of sand [33]. Therefore, LS and LL treatment increased the advancing height of the wetting front.

At the beginning of the test the migration rate of the wetting front was fast and gradually decreased to zero as time proceeded [34]. At the initial stages of the test the migration rate followed the treatment sequence: CK>LS>LL due to failure of the wetting front to rise to the treatment layer at the initial stages of the test. The overlying layer in the control was sand only, that in the LS treatment was both loess and sand, and that of treatment LL was loess only. Due to the low density of loess the weight of overlying soil was small and there was little compaction of the underlying sand. The degree of soil compaction will strongly affect the balance between soil and water [35]. The greater the degree of soil compaction, the greater the migration rate of the wetting front [32]. Capillary porosity affects the rise of soil capillary water [36]. The loess layer has developed pores and good connectivity, forming a path conducive to the rise of capillary water. Therefore, in the later stage of the test, the migration rate of LL and LS treatment is basically greater than that of CK group, and may also be related to the soil water potential on the contact surface (sand-loess interface or loess-sand interface). When there is a composite structure (sand-soil-sand or soil-sand-soil) in the soil profile there will be a clear and sudden change in the water energy at the sand interface which will change the soil water potential and change the water migration rate and water holding capacity of the upper soil [37].

By monitoring the water distribution law of the soil profile after continuous water supply and drainage it was found that LS and LL treatments significantly increased the soil volumetric water content

in the treatment layer (40-60 cm). The thicker the loess interlayer, the greater the volume water content, and the volumetric water content did not decrease after drainage (Fig. 6 and Fig. 7). Studies indicate that the loess layer 10-30 cm under the vegetation rooting zone of the soil can significantly increase the soil water content of the rooting zone [38], and this is consistent with our results here. Because soil texture determines soil water retention and hydraulic characteristics to a certain extent such as soil water retention curve and permeability, different soil textures have important impacts on water distribution in the soil profile [14]. In general, the finer the soil texture the greater its porosity and water retention capacity [39]. Therefore, the soil volumetric water content of LS and LL treatments at 40-60 cm was significantly higher than that of the control, and the thicker the loess interlayer the greater the volumetric water content. In addition, after two months of drainage the volumetric water content in the loess layer treatment (LS and LL) did not decrease, while that in the control decreased by 1.36%. In the presence of a loess interlayer the hydraulic characteristics of the soil profile are discontinuous, leading to a large difference between the soil profile and homogeneous sand [14]. Through measurement and numerical simulation it is found that a layered soil profile can store more water than homogeneous soil under drainage conditions [40] because the structure of the layered soil profile can hinder the vertical movement of water [41]. This shows that when loess is used as an interlayer of sand the treated layer can increase soil water content and has higher water retention characteristics.

However, when the soil profile is constructed artificially the laws governing the movement of water and solutes become more complex because of the discontinuity of the soil profile. Therefore, future studies should examine the changes at the interface of soils of different textures, introduce energy catastrophe theory, scientifically analyze the laws governing the movement of water and solutes, and account for possible salt accumulation and redistribution.

Conclusions

The indoor soil column test is a simple and effective method to study soil water distribution. Here, loess layers of different thickness changed the water

distribution of the soil profile during the advance of a wetting front and the process of drainage. The main findings are as follows:

(1) In the different treatments, the advancing height of the sand wetting front was a power function with time and the loess interlayer treatment promoted the advancing height of the wetting front. A loess interlayer can significantly increase the soil volumetric water content in the corresponding treatment layer (40–60 cm). The thicker the loess interlayer the greater the soil volume water content of the corresponding treatment layer.

(2) After two months of soil drainage the volumetric water content in the corresponding treatment layer (40–60 cm) of a loess interlayer treatment did not decrease significantly, but that of the control decreased by 1.36%.

The results provide a scientific basis and theoretical support for the artificial construction of layered soil profiles to improve the ecological status of sand during the land reclamation of arid and semi-arid mining areas.

Acknowledgments

This study is supported by the National Natural Science Foundation of China (No. 51974326, No. 51574253) and the Capital Science and Technology Talents Training Project (Beijing) (No. Z18110006318021).

Conflict of Interest

The authors declare no conflict of interest.

References

- ZHANG J., WU Q., MA W.P., DU Y.Z., TU K. Integrating the hierarchy-variable-weight model with collaboration-competition theory for assessing coal-floor water-inrush risk. *Environmental Earth Sciences*, **78** (6), 205, **2019**.
- LI B., WU Q. Catastrophic Evolution of Water Inrush from A Water-Rich Fault in Front of Roadway Development: A Case Study of The Hongcai Coal Mine. *Mine Water and the Environment*, **38** (2), 421, **2019**.
- ZHANG X.R., BAI Z.K., CAO Y.G., ZHAO Z.Q., LU Y.Q., PAN J. Ecosystem evolution and ecological storage in outside open-pit mining area. *Acta Ecologica Sinica*, **36** (16), 5038, **2016**.
- LIU W.Q., CHEN, G.Z. Evolution of ecosystem service value and ecological storage estimation in huainan coal mining area. *Bulletin of Environmental Contamination and Toxicology*, **107** (6), 1243, **2021**.
- BI Y.L., PENG S.P., DU S.Z. Technological difficulties and future directions of ecological reconstruction in open pit coal mine of the arid and semi-arid areas of Western China. *Journal of China Coal Society*, **46** (5), 1355, **2021**.
- KAHLOWN M.A., ASHRAF M., ZIA-ul-Haq. Effect of shallow groundwater table on crop water requirements and crop yields. *Agricultural Water Management*, **76** (1), 24, **2005**.
- GAO X.Y., BAI Y.N., HUO Z.L., XU X., HUANG G.H., XIA Y.H., STEENHUIS, T.S. Deficit irrigation enhances contribution of shallow groundwater to crop water consumption in arid area. *Agricultural Water Management*, **185**, 116, **2017**.
- WU X., ZHENG X.J., LI Y., XU G.Q. Varying responses of two *Haloxylon* species to extreme drought and groundwater depth. *Environmental and Experimental Botany*, **158**, 63, **2019**.
- WÖSTEN J.H.M., PACHEPSKY Y.A., RAWLS W.J. Pedotransfer functions: bridging the gap between available basic soil data and missing soil hydraulic characteristics. *Journal of Hydrology*, **251**, 123, **2001**.
- PATRA S., JULICH S., FEGER K.H., JAT M.L., JAT H., SHARMA P.C., SCHWARZEL K. Soil hydraulic response to conservation agriculture under irrigated intensive cereal-based cropping systems in a semiarid climate. *Soil and Tillage Research*, **192**, 151, **2019**.
- LI B.B., LI P.P., ZHANG W.T., JI J.Y., LIU G.B., XU M.X. Deep soil moisture limits the sustainable vegetation restoration in arid and semi-arid Loess Plateau. *Geoderma*, **399**, 115122, **2021**.
- CHU X.J., HAN G.X., XING Q.H., XIA J.Y., SUN B.Y., LI X.G., YU J.B., LI D.J., SONG W.M. Changes in plant biomass induced by soil moisture variability drive interannual variation in the net ecosystem CO₂ exchange over a reclaimed coastal wetland. *Agricultural and Forest Meteorology*, **264**, 138, **2019**.
- ARNETH A., KELLIHER F.M., MCSEVENY T.M., BYERS J.N. Net ecosystem productivity, net primary productivity and ecosystem carbon sequestration in a *Pinus radiata* plantation subject to soil water deficit. *Tree Physiology*, **18** (12), 785, **1998**.
- LI X.P., CHANG S.X., SALIFU K.F. Soil texture and layering effects on water and salt dynamics in the presence of a water table: a review. *Environmental Reviews*, **22** (1), 41, **2014**.
- PHILLIPS J.D. Contingency and generalization in pedology, as exemplified by texture-contrast soils. *Geoderma*, **102**, 347, **2001**.
- ODDIE T.A., BAILEY A.W. Subsoil thickness effects on yield and soil water when reclaiming sodic minespoil. *Journal of Environmental Quality*, **17** (4), 623, **1988**.
- SADEGH-ZADEH F., SEH-BARDAN B.J., SAMSURI A.W., MOHAMMADI A., CHOROM M., YAZDANI G.A. Saline soil reclamation by means of layered mulch. *Arid Land Research and Management*, **23** (2), 127, **2009**.
- FULTON J.P., WELLS L.G. Evaluation of a mechanical system for reconstructing soil on surface mined land. *Applied Engineering in Agriculture*, **21** (1), 43, **2005**.
- AKUDAGO J.A., NISHIGAKI M., CHEGBELEH L P., KOMATSU M., ALIM M.A. Capillary cut design for soil-groundwater salinity control. *Journal of the Faculty of Environmental Science and Technology Okayama University*, **14** (1), 17, **2009**.
- YAN C.G., WAN Q., XU Y., XIE Y.L., YIN, P.J. Experimental study of barrier effect on moisture movement and mechanical behaviors of loess soil. *Engineering Geology*, **240**, 1, **2018**.
- WALTER M.T., KIM J.S., STEENHUIS T.S., PARLANGE J.Y., HEILIG A., BRADDOCK R.D., SELKER J.S., BOLL J. Funneled flow mechanisms in a sloping layered soil: Laboratory investigation. *Water Resources Research*, **36** (4), 841, **2000**.

22. GUO G., ARAYA K., JIA H., ZHANG Z., OHOMIYA K., MATSUDA J. Improvement of Salt-affected Soils, Part I: Interception of Capillarity. *Biosystems Engineering*, **94** (1), 139, **2006**.
23. ZHANG H.Y., LU C., PANG H.C., LIU N., ZHANG X.L., LI Y.Y. Straw layer burial to alleviate salt stress in silty loam soils: Impacts of straw forms. *Journal of Integrative Agriculture*, **19** (1), 265, **2020**.
24. DONG S.N., XU B., YIN S.X., HAN Y., ZHANG X.D., DAI Z.X. Water Resources Utilization and Protection in the Coal Mining Area of Northern China. *Scientific Reports*, **9**, 1214, **2019**.
25. HUANG L., ZHANG P., HU Y.G., ZHAO Y. Vegetation and soil restoration in refuse dumps from open pit coal mines. *Ecological Engineering*, **94**, 638, **2016**.
26. WU Z.Z., YING Y.Q., ZHANG Y.B., BI Y.F., WANG A.K., DU X.H. Alleviation of drought stress in *Phyllostachys edulis* by N and P application. *Scientific Reports*, **8**, 228, **2018**.
27. ZHANG X.L., GUAN T.Y., ZHOU J.H., CAI W.T., GAO N.N., DU H., JIANG L.H., LAI L.M., ZHENG Y.R. Groundwater Depth and Soil Properties Are Associated with Variation in Vegetation of a Desert Riparian Ecosystem in an Arid Area of China. *Forests*, **9** (1), 34, **2018**.
28. XIAO Y., GU X.M., YIN S.Y., SHAO J.L., CUI Y.L., ZHANG Q.L., NIU Y. Geostatistical interpolation model selection based on ArcGIS and spatio-temporal variability analysis of groundwater level in piedmont plains, northwest China. *SpringerPlus*, **5**, 425, **2016**.
29. SHEN R., PENNELL K.G., SUUBERG E.M. Influence of Soil Moisture on Soil Gas Vapor Concentration for Vapor Intrusion. *Environmental Engineering Science*, **30** (10), 628, **2013**.
30. LIU T., JIANG C.L., GUO Y., LI Y.Q., CHENG H. Effect of fly ash content on capillary water rise law in sandy soil. *Journal of China Coal Society*, **41** (11), 2836, **2016**.
31. ZHANG X.D., LIU S.W., WANG Q., WANG G., LIU Y.F., PENG W., XU X.C., LIU Y.W. Experimental Investigation of Water Migration Characteristics for Saline Soil. *Polish Journal of Environmental Studies*, **28** (3), 1495, **2019**.
32. CUI Z.Z., JING X., HAO J.X., DOH S. Analysis of Capillary Water Migration Law of Compacted Loess in Ningxia. *Polish Journal of Environmental Studies*, **30** (1), 61, **2021**.
33. LIU D., LU C.W., LIAN M.J., GU Q.H. Experiment on tailings capillary characteristics based on particle size effect. *The Chinese Journal of Nonferrous Metals*, **30** (11), 2746, **2020**.
34. SEO D., SON Y., BONG T. Model of resalinization by capillary rise in reclaimed land. *Paddy and Water Environment*, **16** (1), 71, **2018**.
35. LEVY M.A., CUMMING J.R. Development of Soils and Communities of Plants and Arbuscular Mycorrhizal Fungi on West Virginia Surface Mines. *Environmental Management*, **54** (5), 1153, **2014**.
36. HALECKI W., KLATKA S. Long term growth of crop plants on experimental plots created among slag heaps. *Ecotoxicology and Environmental Safety*, **147**, 86, **2018**.
37. YAN C.G., ZOU Q., XU Y., WAN Q., SHI Y.L., MA G.F. Water migration rule of loess subgrade with sand interlayers. *Journal of Traffic and Transportation Engineering*, **16** (6), 21, **2016**.
38. WANG Q.M., DONG S.N., WANG H., YANG J., WANG X.D., ZHAO C.H., ZHANG X.Y. Influence of mining subsidence on soil water movement law and its regulation in blown-sand area of Western China. *Journal of China Coal Society*, **46** (5), 1532, **2021**.
39. TIETJE O., HENNINGS V. Accuracy of the saturated hydraulic conductivity prediction by pedo-transfer functions compared to the variability within FAO textural classes. *Geoderma*, **69** (1-2), 71, **1996**.
40. HUANG M.B., BARBOUR S.L., ELSHORBAGY A., ZETTL J.D., SI B.C. Infiltration and drainage processes in multi-layered coarse soils. *Canadian Journal of Soil Science*, **91**, 169, **2011**.
41. ZORNBERG J.G., BOUAZZA A., MCCARTNEY J.S. Geosynthetic capillary barriers: current state of knowledge. *Geosynthetics International*, **17** (5), 273, **2010**.